NBER WORKING PAPER SERIES

UNCERTAINTY, CLIMATE CHANGE AND THE GLOBAL ECONOMY

David von Below
Torsten Persson

Working Paper 14426
http://www.nber.org/papers/w14426

NATIONAL BUREAU OF ECONOMIC RESEARCH
1050 Massachusetts Avenue
Cambridge, MA 02138
October 2008

We are grateful for comments from Eva Benz, Simon Dietz, Daniel Johansson, Karl-Göran Mäler, Will Steffen, Marty Weitzman, and participants in seminars at IIES, MISU, Copenhagen and Mannheim. Financial support from Mistra, the Swedish Research Council, and Jan Wallander and Tom Hedelius' Research Foundation is gratefully acknowledged. The views expressed herein are those of the author(s) and do not necessarily reflect the views of the National Bureau of Economic Research.

Uncertainty, Climate Change and the Global Economy
David von Below and Torsten Persson
NBER Working Paper No. 14426
October 2008
JEL No. E17,O13,Q54

ABSTRACT

The paper illustrates how one may assess our comprehensive uncertainty about the various relations in the entire chain from human activity to climate change. Using a modified version of the RICE model of the global economy and climate, we perform Monte Carlo simulations, where full sets of parameters in the model's most important equations are drawn randomly from pre-specified distributions, and present results in the forms of fan charts and histograms. Our results suggest that under a Business-As-Usual scenario, the median increase of global mean temperature in 2105 relative to 1900 will be around 4.5°C. The 99 percent confidence interval ranges from 3.0 °C to 6.9 °C. Uncertainty about socio-economic drivers of climate change lie behind a non-trivial part of this uncertainty about global warming.

David von Below
Institute for International Economic Studies
Stockholm University
106 91 Stockholm, Sweden
belowd@iies.su.se

Torsten Persson
Director
Institute for International Economic Studies
Stockholm University
S-106 91 Stockholm
SWEDEN
and NBER
Torsten.Persson@iies.su.se

1 Introduction

Uncertainty about future climate change is an unavoidable fact. It is commonplace to gauge this uncertainty by simulations with different climate models. This is the approach taken, e.g., by the International Panel on Climate Change (IPCC, 2001, 2007) to highlight our imprecise knowledge about the relation between specific atmospheric concentrations of greenhouse gases (GHGs) and global temperature. These model simulations typically rely on a small set of common and deterministic emission scenarios, so-called SRES-storylines (Nakićenović *et al*, 2000), which are not related to the processes underlying economic growth and energy use in an explicit and reproducible way.[1] The approach is thus a partial one, focusing on specific biogeophysical relations in the complicated chain from human activity to climate change (and back). However, the socioeconomic relations behind regional and global economic growth, energy use and emissions are equally fraught with uncertainty as the biogeophysical relations.

A comprehensive assessment of the uncertainties about the important links in the chain from economic conditions to climate change is obviously a monumental task, and this paper is merely a first pass at the problem. Our approach is to simultaneously introduce uncertainty about a number of parameters that shape exogenous variables and endogenous relationships in the same simple, but comprehensive, model of the global climate and economy. We then perform Monte Carlo simulations, i.e., we make a large number of random draws of the full set of parameters and simulate the entire model for each such draw to derive probability distributions at different points in time for the variables of most interest. Climate sensitivity (the effect on global mean temperature of a doubled GHG concentration) remains the single most important determinant of uncertainty about global warming, but well-identifiable socioeconomic developments – such as population growth, and improvements of overall technology and energy efficiency – drive a non-trivial part of that uncertainty. Closing down uncertainty about climate sensitivity altogether, there remains an uncertainty range of temperature a hundred years from now of about 3 °C.

Conceptually, our analysis is similar to that of Wigley and Raper (2001) who derive a probability distribution for future global mean temperature in a simple climate model, by introducing uncertainty through assigned probability density functions (p.d.f.) for the main drivers of temperature. However, their study stresses uncertainties in the biogeophysical and biogeochemical systems, while emissions are given by a (uniform) p.d.f. over alternative SRES scenarios, rather than alternative socioeconomic developments. A similar analysis is performed in the PAGE model (Hope, 2006) used in the

[1] For a broad, and critical, discussion of the SRES methodology see McKibbin, Pearce and Stegman (2004) or Schenk and Lensink (2007). Webster *et al.* (2002) and Mastrandrea and Schneider (2004) discuss the use of scenarios vs. a probabilistic approach.

Stern Review (Stern, 2006). Analogously, Murphy *et al.* (2004) derive a probability distribution for climate sensitivity from the Hadley Centre climate model, by drawing alternative values of the parameters that govern the model's important relations. Mastrandrea and Schneider (2004) use the DICE model, an aggregated version of the RICE model used in this paper, to produce probability distributions for temperature increase. Aspects of their methodology is close to ours, but the analysis concerns optimal climate policy and focuses on uncertainty about climate sensitivity rather than socio-economic drivers of climate change. Nordhaus and Popp (1997) do consider uncertainty about socioeconomic drivers of climate change, but their purpose is again different (to gauge the value of different types of scientific information). Finally, Webster *et al.* (2002) derive GHG emission scenarios in a probabilistic manner, by introducing uncertainty over important variables in an economic model.

Our analysis relies on a slightly modified version of RICE, an integrated model of climate and growth, developed and described by Nordhaus and Boyer (2000). Section 2 gives a short description of that model and our modifications of it. Section 3 explains how we introduce uncertainty about model parameters. Section 4 presents results for variables of interest in two forms: fan charts, which illustrate how uncertainty develops over time, and histograms, which illustrate uncertainty at a point in time 100 years from now. Section 5 concludes.

2 The modified RICE model

We need a model that incorporates the global economy as well as the climate system and allows us to parametrically vary assumptions about important relations. For these reasons, we use an adapted version of the RICE–99 model, as formulated in Appendix D of Nordhaus and Boyer (2000).[2] Next, we provide an overview of this model and our modifications. Equation numbers, variables, and parameters in brackets refer to a formal description of the model in the Appendix.

General description of RICE–99. The world is divided into eight regions (indexed by J) on the basis of geography as well as levels of economic development: United States (USA), OECD Europe (EUR), Other High Income countries (OHI), Russia and Eastern Europe (REE), Middle Income (MI), Lower Middle Income (LMI), China (CHI) and Lower Income (LI).[3] Neither trade nor investments flow between regions. Time (indexed by t) is measured in 10-year periods, starting in 1995. In each period, each region

[2]This monograph gives a general description of the RICE model (chapter 2), and its appendix (pp. 179-187) includes all equations and parameter values of the baseline model.

[3]See Nordhaus and Boyer (2000) pp. 28–38 for definitions of regions.

produces a homogeneous good with a neoclassical production technology based on capital and labor, but augmented by "energy services" reflecting the carbon content of energy inputs (see equation A.4). Regional damages from climate change are modelled as an output loss proportional to the value of GDP.

Economic growth in each region is driven by growth of population (A.5) and total factor productivity (TFP) (A.6). Higher economic growth implies more rapidly increasing regional demand for energy. How much this translates into use of exhaustible carbon resources depends on carbon-saving technological change (A.7), as well as regional energy prices. These prices have a regional component, reflecting regional taxes and distribution costs, and a global component, reflecting gradual exhaustion of the finite global supplies of oil, coal and natural gas (A.10–A.12). Naturally, higher prices curtail energy use.

Energy use in each region and time period creates industrial CO_2 emissions that, together with emissions from changes in land use and changes in the properties of the biosphere, end up in the global atmosphere (A.13). The model incorporates a simple carbon cycle, i.e., carbon flows between atmosphere, biosphere (cum shallow oceans), and deep oceans (A.14). Any CO_2 not absorbed in the ocean sinks adds to atmospheric concentration. Via increased radiation (A.15) more CO_2 raises global-mean surface temperature (A.16) in an amount depending on climate sensitivity.[4] Changes in climate create damages reflecting e.g., lower agricultural productivity, more frequent storms, or resettlements due to coastal flooding (A.17 and A.18). Damages, as a proportion of gross GDP, are region-specific quadratic functions of global temperatures in the period relative to 1900. Larger damages imply lower welfare. They also create a negative feedback effect, whereby lower output growth leads to less energy use ultimately reducing temperature.

Along an equilibrium time path of the model, consumers and producers in each region make decentralized utility and profit-maximizing decisions, adjusting savings and investments to the incomes, interest rates, technologies, and market prices they observe and rationally expect to prevail in the future. In particular, producers adjust their use of carbon-based energy to available technologies and regional energy prices. Regional and global welfare functions (A.1–A.3) are maximized in equilibrium.

RICE can be programmed and solved in two ways. The usual way is to maximize welfare, taking regional damages explicitly into account, so as to derive optimal uses of carbon-based energy, given their adverse effects via global temperature, and to calculate optimal carbon prices. Since our pur-

[4]The climate-sensitivity parameter (κ) captures, in a very simple way, the complicated interactions in the earth system that produces a warmer climate as the atmospheric concentration of GHGs goes up.

pose is different, we do not take damages into account in the maximization. This way, we illustrate future paths in the absence of additional mitigation measures: Business As Usual (BAU) in the jargon of the climate-change literature.

Modifications We make a few adjustments to the RICE model, as follows.

Data for most variables entering the model are now available for the period 1996–2005 so we update initial values by one (ten-year) period and start off in 2005 rather than 1995. Atmospheric temperature for 2005 ($T(0)$ in A.16) comes from the UK Met Office, and atmospheric concentration of CO_2, ($M(0)$ in A.14) is obtained from the Carbon Dioxide Information Analysis Center[5] (CDIAC) and converted into a stock. The concentration of CO_2 in the upper oceans ($M_U(0)$ in A.14) is derived from the latter figure. Initial population figures for 2005 ($L_J(0)$ and $g_J^L(0)$ in A.5) come from the UN *World Population Prospects: The 2004 Revision Population Database*. GDP figures for 2005 are collected from the World Bank's *World Development Indicators* (WDI) database. These are used to calibrate initial levels of TFP, capital stocks, and energy services ($A_J(0)$, $K_J(0)$, and $ES_J(0)$ in A.6–A.9), assuming that investments and energy service inputs were chosen optimally in all regions between 1995 and 2005. Finally, we estimate current values of the TFP and energy efficiency growth rate parameters (equations A.6 and A.7), using data from the Penn World Tables (Heston, Summers and Aten, 2002) and the World Bank's WDI database. The precise numbers assigned to parameters and initial conditions are given in Tables 1 and 3 in the Appendix.

RICE assumes that the rate (all) consumers use to discount the utility of future consumption declines over time; we reset it to a constant. Specific assumptions about the discount rate are very important when using a climate model for the normative (prescriptive) purpose of finding optimal paths of mitigation (because abatement costs close in time are traded off against benefits of lower damages much further away in time).[6] For our specific positive (descriptive) purpose to illustrate uncertainty about future outcomes under BAU assumptions, the discount rate is much less important.

Finally, we try to incorporate scientific findings that the biosphere's ability to absorb CO_2 might change with climate.[7] At some level of CO_2 concentration in the atmosphere, the biosphere will likely switch from being a CO_2 sink to a CO_2 source. (Oceans too may absorb less CO_2 as climate

[5]The latest available figures for CO_2 concentration refer to 2004; linear extrapolation was used to get an estimate for the 2005 value.

[6]The specific assumptions about the discount rate have indeed been one of the major points in the public discussion about the conclusions in the Stern Review (Stern, 2006); see, e.g., Nordhaus (2006), Dasgupta (2007) and Weitzman (2007).

[7]This alteration of the model is based on personal communications with Will Steffen and on Friedlingstein *et al.* (2006).

changes, but these effects are smaller and less certain.) It is estimated that this terrestrial biosphere effect may contribute an additional 40–400 Gigatons of carbon (GtC) into the atmosphere by 2105, most models predicting a number between 100 and 200 GtC.

Ideally, the terrestrial biosphere effect should be added as an additional module to the climate part of the model. We have chosen a simpler solution: we just add an additional flow of emissions into the atmosphere in every period, calibrated to yield an average additional concentration in 2105 corresponding to 150 GtC. However, this value is highly uncertain, so we impose a probability distribution on it, as we do for many other model parameters.[8] The specification of such parameter uncertainties is the topic of the next section.

3 Introducing Uncertainty

We express the uncertainty about individual parameters and exogenous variables in the model as statistical distributions on the forms summarized in Tables 1 and 3. Most distributions are assumed to be Gaussian; the uncertainty about the terrestrial biosphere effect is deemed to be asymmetric and therefore a beta-distributed random variable is used to generate this process. The probability distribution for the climate-sensitivity parameter is a special case derived from a truncated normal distribution, as discussed below.

Means for most parameters are close to the specific parameter values used in RICE, except that we raise the means of initial TFP growth rates to correspond more closely to the growth experience in the last ten years.

Using the p.d.f. of each one of the assumed distributions, we conduct a Monte Carlo simulation with 10001 independent random draws of the full set of parameters. For each of these draws, we carry out a full dynamic simulation for 400 years: an equilibrium time path of the model, as described above. These 10001 equilibrium paths generate different levels of GDP, emissions, temperatures, etc., which we use to describe the uncertainty about these outcomes.

Of course, each assumption regarding the distribution of an underlying parameter is a subjective assessment, made by ourselves or some collective of scientists. Most of the many relations that contribute to the climate problem are highly uncertain, however, and our objective is to illustrate a way

[8] Specifically, these additional emissions are modelled with the following process:

$$TBE\,(t) = (\tau_1 + \tau_2\gamma)(t + \tau_3 t^2),$$

where scalars τ_1, τ_2 and τ_3 and random variable γ have been calibrated so that the terrestrial biosphere effect, on everage, adds 150 GtC in the atmosphere by 2105, with values falling between 40 and 400 GtC.

to take this comprehensive uncertainty into account. We believe that the exercise meaningfully gauges the magnitude of uncertainty at different time horizons. Moreover, it helps illustrate the effects of favorable or unfavorable — from the viewpoint of climate change — circumstances, and which circumstances matter the most. Next, we provide details on the various sources of uncertainty.

Population Population growth is a major source of uncertainty about future output growth. In RICE, regional population trajectories are pinned down by two parameters: initial population growth rates, and the decline rates for population growth ($g_J^L(0)$, and δ_J^L in A.5). To calibrate these parameters, we rely on the UN *World Population Prospects: The 2004 Revision Population Database,* which contains country-level population forecasts in five-year intervals up until 2050 in the form of three different scenarios: *low*, *median* and *high*. We aggregate these country scenarios up to RICE regions, and estimate growth parameters $g_J^L(0)$ and δ_J^L based on the *median* scenarios. Uncertainty about these parameters is estimated using the variability between scenarios, assuming that *high* and *low* represent ± 2 standard deviations around the *median*.[9]

Figure 1 shows the median population trajectories for all regions and confidence bands around them in the form of fan charts.[10]

TFP Along with population growth, productivity growth is the most important determinant of future output levels. Our estimated TFP growth rates, which are higher than in RICE–99, are calculated in the following manner. Country-level investment data from the Penn World Tables and the perpetual inventory method are used to construct a series for capital stock. These figures, along with data on GDP[11] and population, allow us to calculate past TFP levels using a standard Cobb-Douglas production function. In these calculations, we use data for countries where data is available for the whole period 1960–2000, except for REE where no data is available before 1992; here we use 1992–2000.

We then aggregate these data up to RICE regions and five year-periods, and use these to form statistical estimates of TFP growth processes on the functional form used in RICE.[12] Specifically, we estimate initial growth

[9]For most regions, the UN forecasts and their implied uncertainty can be approximated very closely with model parameters. However, for EUR, OHI and CHI, population levels are projected to first rise and then fall. Mean population forecasts and the uncertainty around them are therefore entered manually up until 2045 for these regions.

[10]Throughout the paper, we choose to focus on the time period between now and 150 years ahead in the charts presented; however, the model simulations run through 40 time periods, i.e., 400 years.

[11]Throughout the paper, PPP-adjusted GDP figures have been used.

[12]We perform the statistical analysis on data for five-year periods, for several reasons. First, we are interested in long-term trends in TFP rather than year-to-year changes.

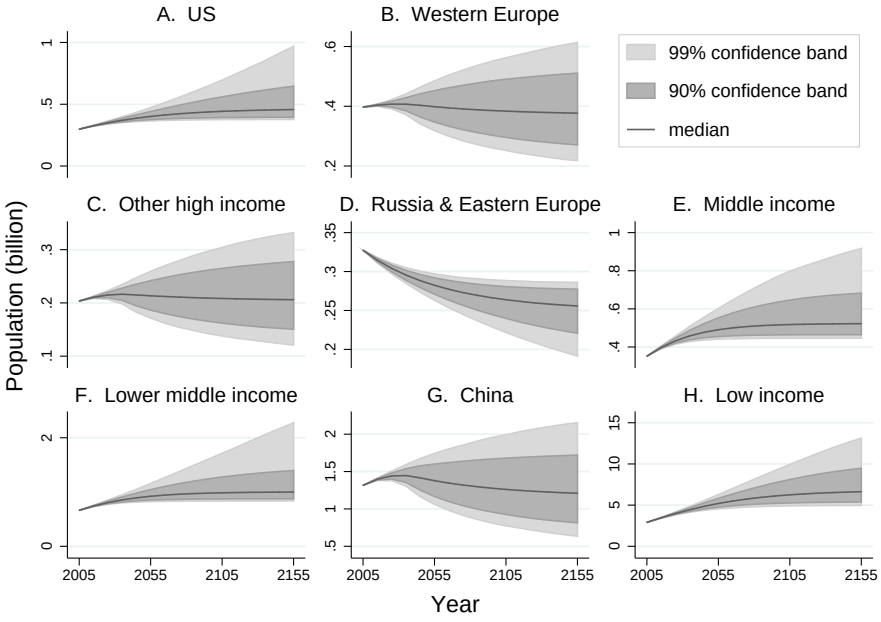

Figure 1: Forecasts for regional population levels, $L_J(t)$

rates of TFP ($g_J^A(0)$) along with two location parameters, using nonlinear least squares. We then draw $g_J^A(0)$ from normal distributions with mean and variance obtained from our statistical estimates. We also impose uncertainty about the steady-state levels for TFP, drawing them from normal distributions, whose means are the steady-state values used in RICE-99, and whose variance is the one we estimate from the data. In each draw underlying our simulations, we use the initial growth rate and the steady state value to back out the implied decline rate for TFP (δ_J^A). [13]

One qualification to the above is that no estimates for $g_J^A(0)$ were obtained for REE: the functional form in RICE doesn't fit the data for this region, since TFP fell throughout most of the 1990s and only recently started

Second, using yearly data would give higher precision in the estimates — but this would be false precision. We only have data for roughly half the countries, and we only observe one history, which makes the TFP process look more smooth and predictable: percieved precision is likely false. Using five-year data helps take this greater uncertainty into account. (For REE, data availability necessitates the use of two-year data.)

[13]The decline rates, δ_J^A, were arrived at as follows. Initial growth rates and the associated decline rates are (empirically) highly correlated, and, more importantly, they jointly determine the steady-state level of TFP. In particular, the expression

$$\exp\left(g_J^A(0)/\delta_J^A\right)$$

defines the steady-state TFP level. Given values for $g_J^A(0)$ and the steady-state level, we can thus back out the implied decline rate δ_J^A.

to rise. Instead, values close to those for China were used for REE.

The regional TFP growth processes are modelled as independent of each other — i.e., in a particular model simulation, say, the US, may have rapid TFP growth while Europe's is slow. If technology spreads easily across countries and regions, one might think that technology shocks should be positively correlated. To address this concern, we have also run a version of the model where the TFP and energy efficiency processes have a (dominating) global component, alongside (less important) regional components. This specification made little difference to the results, but increased substantially the running time of the program. For this reason, we only report results for the simpler specification with independent technological growth processes across regions.

Figure 2 illustrates our TFP forecasts in the form of fan charts (note the different scales on the y-axes).

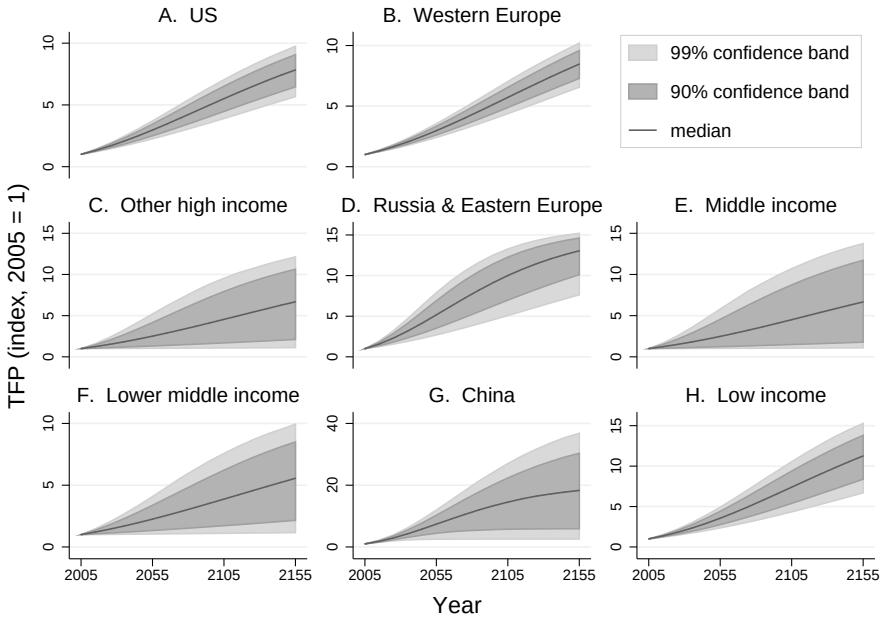

Figure 2: Forecasts for regional TFP levels, $A_J(t)$

Energy efficiency Energy efficiency in production is modelled with parameter $Z_J(t)$, which is set at 1 in all regions in the initial period. Z then declines following a process similar to population and TFP growth, with an initial (negative) growth rate, $g_J^Z(0)$, and a decline parameter, δ_J^Z. A lower value of Z means higher energy efficiency: less CO_2 is emitted for the same amount of carbon energy used. Since energy efficiency is modelled with the same type of process as TFP, we estimate its parameters in an analogous

manner. Exploiting data on the ratio of CO_2 emissions to GDP, carbon intensity, from the World Bank *World Development Indicators* database, we estimate means and standard deviations of initial-period growth rates, as well as uncertainty about steady-state levels, using nonlinear least squares. Data exists from 1980 until 2004, and we use three-year data in our estimations, starting in 1982 (for REE data again exists only from 1992, here we use two-year data starting in 1992).

This works well for all regions except for MI, LMI and LI, where carbon intensity has been rising up until recently. For these regions, a logistic-type functional form is fitted in order to estimate the initial growth rates, $g_J^Z(0)$, and uncertainties about the steady-state levels are assigned roughly the same values as for China. The means of the probability distributions for steady states for all regions are again the same as the ones implied in RICE–99, and we back out the implied δ_J^Z in the same way as for TFP.

Figure 3 shows the forecasts for the energy efficiency parameter $Z_J(t)$. As the figure shows, energy efficiency improvements are expected to be asymmetric in some regions. This is due to truncation of some of the steady-state uncertainty distributions — carbon intensity can never fall below 0.

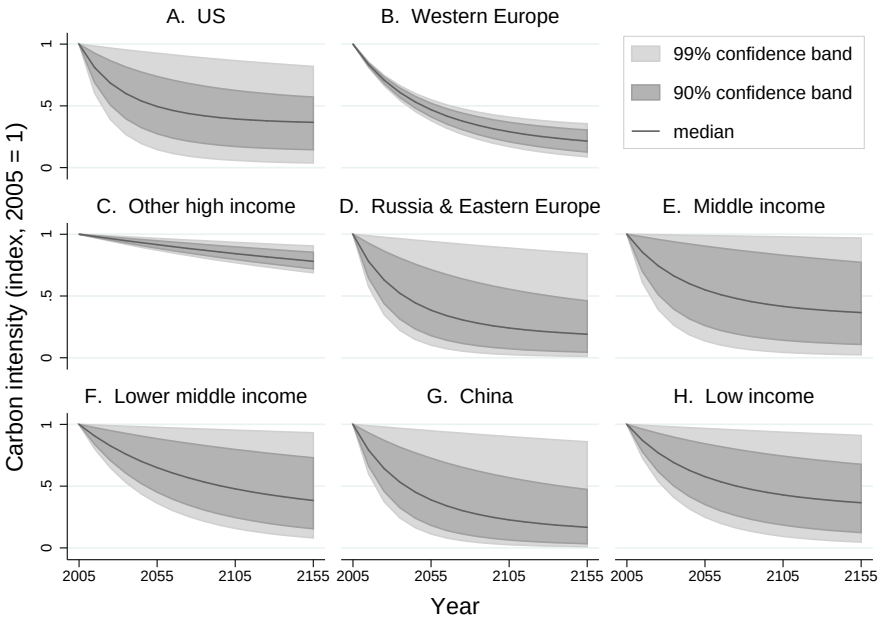

Figure 3: Forecasts for regional energy efficiency, $Z_J(t)$

Land use Emissions of CO_2 due to changes in land use arise mainly from deforestation: carbon of burnt biomass is released as carbon dioxide. In RICE, this process is modeled in similar fashion to other growth processes.

Each region has an initial rate of emissions due to land use changes, and these rates then decline slowly at a rate set at 10% per decade.

We update initial emission rates and introduce uncertainty over them, based on figures in Chapter 7 of the WG1 contribution to the fourth IPCC Assessment Report (IPCC 2007). In particular, we use the disaggregated (Tropical Americas, Africa and Asia) AR4 estimates for the 1990s given in Table 7.2, interpreting the uncertainty ranges as ± 3 standard deviations.[14] The figures for the Lower Middle Income and especially Lower Income regions are revised upwards; for the other regions, changes are minor. Exact figures are reported in Table 3 in the Appendix.

Climate sensitivity The climate sensitivity parameter, κ, measures the rise in temperature following a doubling of atmospheric CO_2 concentrations. Many estimates of this parameter lie in the region around 3.0, but uncertainty about the true value is substantial and many climate models generate an asymmetric distribution. As explained by Roe and Baker (2007), a distribution with a pronounced right tail is a natural outcome of uncertainty about the various feedback processes whereby higher temperatures raise the level of radiative forcing. Examples of such feedbacks are changes in the formation of water vapor and clouds, or in the earth's albedo (ability to reflect solar radiation). In the RICE model framework, it is natural to portray the uncertainty about such feedbacks as uncertainty about climate sensitivity. We generate the latter following the same reduced-form approach as Roe and Baker. In their notation, we set (the average value and standard deviation of the feedback parameter) $f = 0.65$ and $\sigma = 0.10$, and in order to avoid extremely high (even infinite) values for κ, we truncate the distribution by cutting off 1% in the upper tail.[15] Passing this truncated normal through the highly nonlinear transformation illustrated in Roe and Bakers's Figure 1, we obtain a p.d.f. similar in shape to the weighted p.d.f. reported in Figure 3 of Murphy *et al.* (2004).[16] The mean and median of this theoretical distribution are about 3.71 and 3.41 respectively. Figure 4 plots the frequency of draws, the realized p.d.f. for κ, used in our simulations.

Other uncertainties As mentioned above, we use a constant rate of time preference (ρ). The discount rate is assumed to have a normal distribution

[14] We take Lower Income countries to correspond to Tropical Africa and most of Tropical Asia, attributing the remaining fractions of the figure for Asia to Malaysia, which counts as Middle Income, and to China. The figure for Tropical Americas is divided equally between Middle Income (Brazil) and Lower Middle Income (most other Latin American countries).

[15] This means that we are excluding the possibility of "runaway climate change"— where feedback effects reinforce each other, resulting in a chaotic and entirely unpredictable climate. Such futures are not readily incorporated into the RICE framework.

[16] For Roe and Baker's ΔT_0, which they refer to as climate sensitivity in the absence of feedbacks, we use the value 1.2 °C.

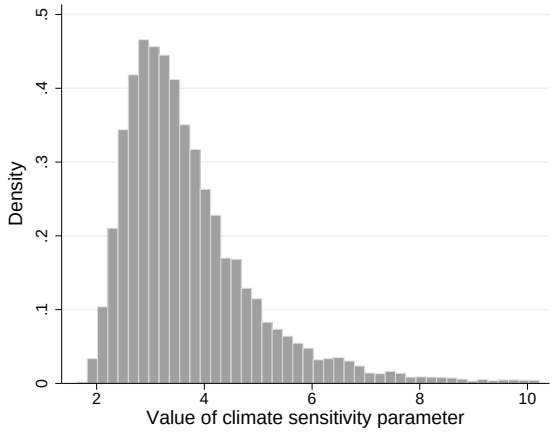

Figure 4: Distribution of draws on κ

with standard deviation 0.33 around an average value of 3% (the initial rate in RICE). This way, random draws almost always fall within the range $[2, 4]$ with most outcomes within $[2.5, 3.5]$.

Uncertainties about the regional coefficient on carbon-energy in the production function (β_J), the damage function parameters ($\theta_{1,J}$ and $\theta_{2,J}$), and the global carbon supply parameters (ξ_2, ξ_3 and $CMAX$) were found to play a very minor role the exercise carried out here. To keep matters simple, these parameters were assigned normal distributions with standard deviations 20% of their mean values.

4 Results

This section reports on selected results from our Monte Carlo simulations. To keep the presentation short, we focus here on the global variables of most interest.

World GDP Figure 5 shows future values of (the logarithm of) world GDP, measured in trillion USD (in 1990 prices).

Panel A illustrates the uncertainty with a fan chart, showing the median realization plus 90 and 99% confidence bands over the coming 150 years. Panel B shows a histogram of estimated world GDP 100 years ahead, which corresponds to an (unsmoothed) p.d.f. for that variable. Most of the uncertainty about future GDP levels stems from variability in TFP growth.[17] But variability in population growth and other exogenous parameters mat-

[17] A Regression of world GDP in 2105 on the realizations of all 16 TFP growth parameters within the same Monte Carlo draw gives an adjusted R-square of 0.567

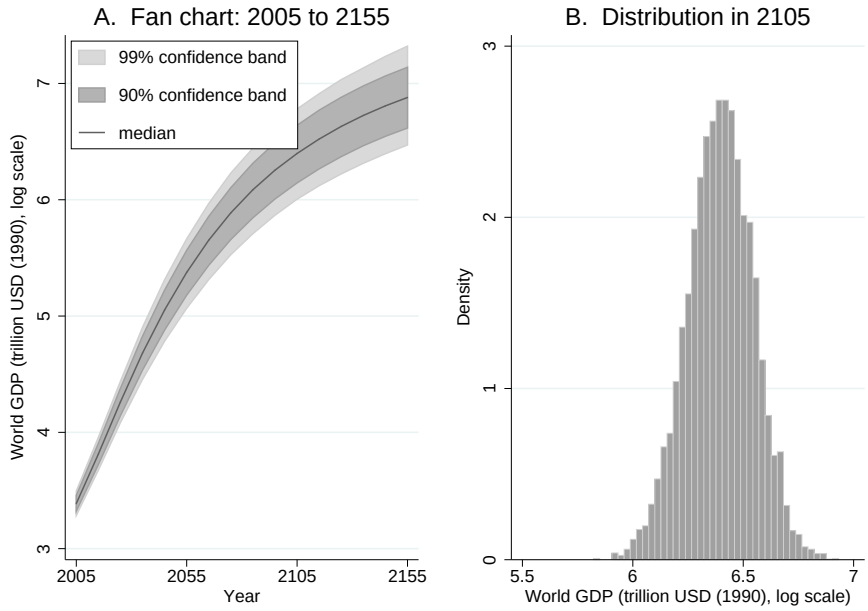

Figure 5: World GDP projections

ters too, as does the fact that we report word GDP *net of* damages caused by rising global temperatures (as defined in A.17 and A.18).

Inspection of the simulation data reveals that the realizations in the right tail of the world GDP distribution are due to some combination of high growth rates in the US, China or low-income countries; the US because of its high initial GDP level, and the latter two because of their population size.

Industrial emissions Since production requires carbon energy as an input, higher GDP generally means higher industrial CO_2 emissions. However, substantial gains in energy efficiency allow incomes to grow without corresponding growth in emissions. Figure 6 illustrates future carbon emissions, measured in GtC. As the fan chart shows, uncertainty increases steadily over time, reflecting the increasing uncertainty about economic growth and energy efficiency. Annual emissions in the median BAU realization reach their maximum some fifty years ahead, at about three times their current level just below 10 GtC per year. Emissions then start to decline slowly, because carbon-saving technological change and the effect of higher carbon prices eventually outweigh the increased demand from higher world production. The upper part of the fan chart shows that in 500 of our 10001 simulations (i.e., 5%) industrial emissions peak at more than five times their current level.

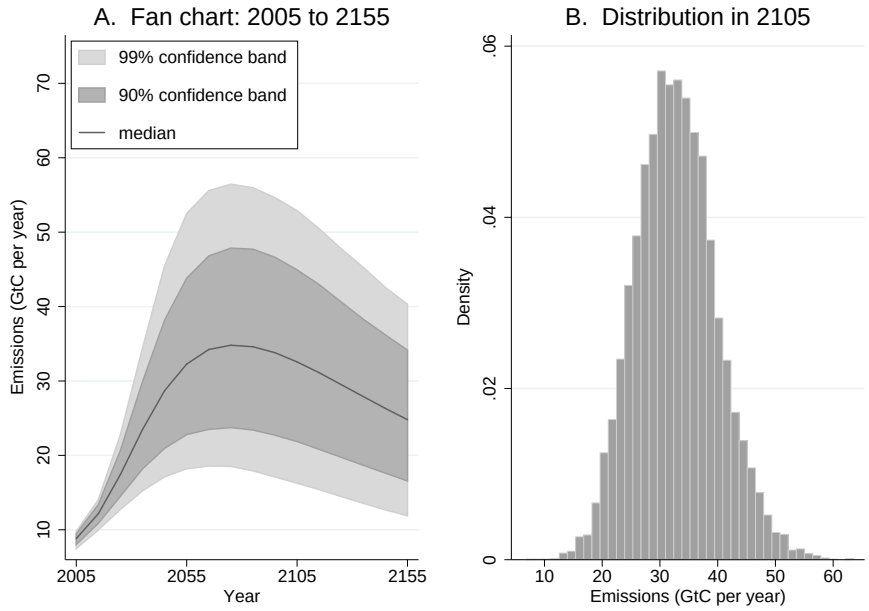

Figure 6: Projections for industrial emissions of CO_2

The 2105 histogram illustrates an upward skew in the emissions distribution. The data shows that the extreme realizations in the right tail come about when either China or the group of low-income countries experience large increases in GDP growth but little improvement in energy efficiency. This is intuitive, given the population size of these regions, and their relatively poor initial energy efficiency.

Atmospheric CO_2 concentration Because emissions, even in the low-growth BAU paths, are far larger than the earth's natural absorption capacity, they keep adding to the atmospheric concentration of CO_2 measured in parts per million (ppm). This is illustrated in Figure 7.

In the model, industrial CO_2 emissions are closely linked to atmospheric concentration of carbon dioxide. The two are not perfectly correlated, however, given the uncertain terrestrial biosphere effect and uncertain regional changes in land use. Nevertheless, extreme values for CO_2 concentrations reflect the same causes as high industrial emissions. Since the carbon cycle is a slow process, the atmospheric concentrations adjust to emissions only with a long time lag, so we do not see a slowdown in CO_2 concentration growth following the peak in emissions within the time frame of the fan chart.

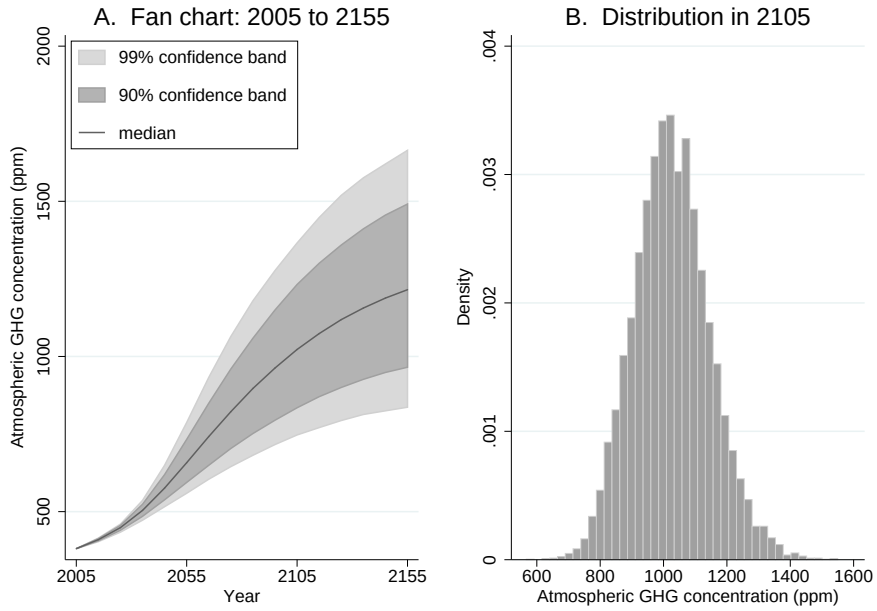

Figure 7: Projections for atmospheric GHG concentration

Global warming Figure 8 shows future increases in global mean surface temperatures, relative to the year 1900, measured in Centigrades (°C). A century from now, the median realization of temperature is around 3.8 °C above today's temperature, which, in turn, is 0.71 °C above the 1900 level. Such median temperature hike is broadly consistent with the median 2.5 fold increase of CO_2 concentration in Figure 7, and a median climate sensitivity of approximately 3.4.[18]

What causes variability of global temperature in our simulations? The climate sensitivity parameter, κ, is the most important source of uncertainty.[19] This reflects the fact that climate sensitivity is the last link (in the RICE model) in the chain from human activity to global warming. In 2105, the 99% confidence interval for temperature is almost 4 °C wide. This range of warming for the next century is of the same magnitude as the range reported elsewhere, but derived with very different methods (see e.g., IPCC

[18]Climate sensitivity refers to the long-run effect on temperature of a doubled CO_2 concentration, which is reached only with considerable time lag. This makes the actual rise in temperature between 2005 and 2105 fall short of 4.2 °C even though the concentration of CO_2 would increase by a factor of 2.5 in that time. On the other hand, the model's temperature hike from 2005 to 2105 also incorporates lagged reactions to higher CO_2 concentrations before 2005. This adds an additional boost to 2105 temperature, above the value implied by the addition to CO_2 concentration between 2005 and 2105.

[19]A regression of temperature increase in 2105 on values of draws on κ gives an adjusted R-square of 0.76.

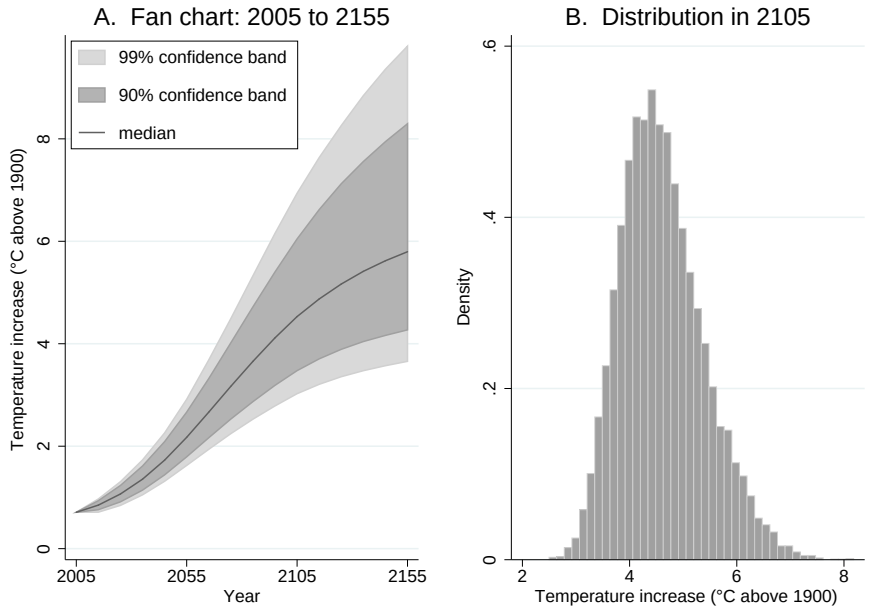

Figure 8: Projections for temperature increase

2001, 2007).

Notice that already the 5^{th} percentile in Figure 8 lies clearly above 2 °C of warming in fifty years' time. Indeed, the histogram in panel B shows that all of the 10001 temperature realizations a century from now lie above 2 °C, which is considered by the European Union as the upper limit for such a manageable climate change as referred to in Article 2 of the UNFCCC. Even the most optimistic realizations in the leftmost tail for temperature should thus be a matter of grave concern.

Anyone who pays close attention to the optimistic tail, should seriously consider also the pessimistic tail of the distribution for climate change. As the histogram in Figure 8 shows, the highest temperature realizations by 2105 involve a rise above 7 °C. As is well-known the effects of such temperature changes are very hard to predict, but may include eventual sea levels high enough to threaten major cities as London, Shanghai, or New York, and substantial risks of large-scale shifts in the Earth system, such as collapses of the Gulf Stream or the West Antarctic ice sheet.

What realizations of the future lie behind the most severe instances of global warming? As already mentioned, climate sensitivity above its mean is a very important one. But other reasons are more squarely rooted in the human system. One is lower than expected improvements of energy efficiency in regions with high production and dirty technologies: chiefly the US and China. Another root is higher than expected economic growth in

very populous regions, in particular the current low-income countries that host about half of the world population. To put it bluntly, futures in which today's unfortunate manage to permanently break out of poverty (without large improvements in energy-saving technologies) have substantially higher global warming. Ironically, resolution of one of today's most pressing global problems aggravates another one.

Figure 9 illustrates the interplay between different sources of climate change.[20] Panel D plots the temperature increase a hundred years from now against the randomly drawn value of the climate-sensitivity parameter (κ). A log curve approximates the relationship well, but the variability around this curve stems from variation in other parameters. We use the four highlighted observations, labeled 1 through 4 in all plots, to discuss how (sources of) GDP growth and energy efficiency matter for climate change. (Note that the temperature axis has the same scale in all four plots.)

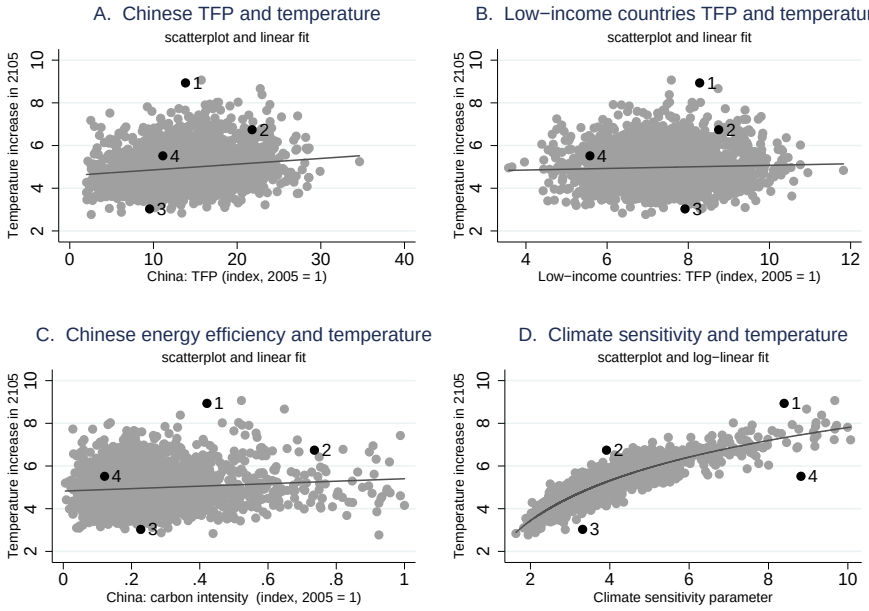

Figure 9: Illustration of sources of variability.

Observation 1 is the most extreme outlier on the upside, and has the second-highest temperature increase, around 8.9 °C. Climate sensitivity is high, but temperature is still well above the fitted curve in the bottom right plot. This result is driven mainly by relatively low improvements in energy efficiency in several of the world's poorer regions (MI, LMI, CHI) — China's carbon intensity, shown in panel C, is at the 87$^{\text{th}}$ percentile

[20]To make it easier to see the density of the scatterplots, Figure 9 displays a random draw of 2001 (out of 10001) observations.

among the 10001 simulations (recall that less pollution corresponds to lower values of carbon intensity). Observation 2 has a temperature more than 6.5 °C above pre-industrial. This is due to how China develops: relatively high Chinese TFP growth interacts with one of the lowest improvements in Chinese energy efficiency (98^{th} percentile). Low-income countries' TFP is also well above average. The low temperature increase in observation 3 is due to relatively low GDP growth in the world's two most populous regions, China and the group of low-income countries. In the latter region this is due to low population growth; in China the reason is low improvements in TFP. Observation 4 has about 2 °C lower temperature than what climate sensitivity predicts — and about 3 °C less than observation 1, with roughly the same climate sensitivity. The reasons are substantial improvements in energy efficiency in most regions, along with below-average TFP growth in China and especially low-income countries (7^{th} percentile).

These alternative futures illustrate that alternative socioeconomic developments contribute a great deal to the uncertainty about future global warming. Figure 10 illustrates this further, by showing the result of a Monte Carlo simulation with 10001 draws, where climate sensitivity is held constant at its mean value. A hundred years from now, the range for temperature outcomes is about 3 °C wide and the highest temperatures are well above 6 °C. The 99% confidence interval is 1.8 °C wide, to be compared with a corresponding confidence interval of 3.9 °C when we allowed for uncertain climate sensitivity in Figure 8.

Figure 10: Temperature projections under certain climate sensitivity

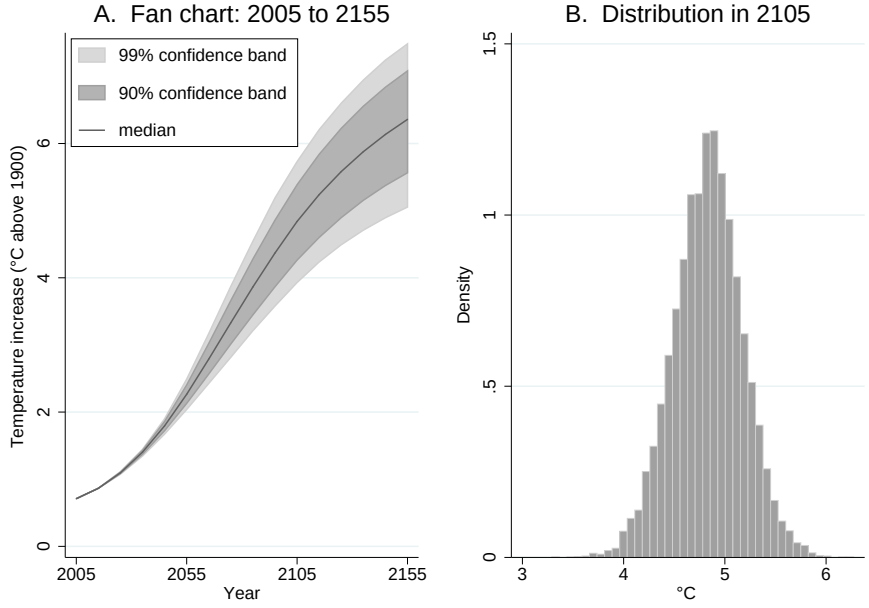

5 Conclusions

On the methodological side, our paper illustrates a way forward in analyzing uncertainty about future climate change, which includes the most important determinants in the human system as well as the natural system. Our results suggest that uncertainties about relations in the economic system can play a major role. More research, with less stylized assumptions and more comprehensive climate-economy models, should follow.

On the substantive side, our simulations rely on BAU assumptions regarding energy taxes and other means of mitigating climate change. Absent future mitigation efforts, global warming will be substantial even under very favorable circumstances.

Appendix

This Appendix begins with a list of the full set of equations in the underlying RICE model. It also includes a list of all the model's variables and the distributions for the parameters we use in the Monte Carlo simulations.

RICE model equations

(A.1) $W_J = \sum_t U[c_J(t), L_J(t)]R(t)$

(A.2) $R(t) = \prod_t [1+\rho]^{-10t}$

(A.3) $U[c_J(t), L_J(t)] = L_J(t)\{log[c_J(t)]\}$

(A.4) $Q_J(t) = \Omega_J(t)\left\{A_J(t)K_J(t)^{\alpha}L_J(t)^{1-\beta_J-\alpha}ES_J(t)^{\beta_J} - c_J^E(t)ES_J(t)\right\}$

(A.5) $g_J^L(t) = g_J^L(0)\exp(-\delta_J^L t),\ g_J^L(0)$ given

$L_J(t) = L_J(0)\exp\left[\int_0^t g_J^L(t)\right],\ L_J(0)$ given

(A.6) $g_J^A(t) = g_J^A(0)\exp(-\delta_J^A t),\ g_J^A(0)$ given

$A_J(t) = A_J(0)\exp\left[\int_0^t g_J^A(t)\right],\ A_J(0)$ given

(A.7) $ES_J(t) = Z_J(t)E_J(t)$

$g_J^Z(t) = g_J^Z(0)\exp(-\delta_J^Z t),\ g_J^Z(0)$ given

$Z_J(t) = Z_J(0)\exp\left[\int_0^t g_J^Z(t)\right],\ Z_J(0) = 1$

(A.8) $Q_J(t) = C_J(t) + I_J(t)$

$c_J(t) = C_J(t)/L_J(t)$

(A.9) $K_J(t) = K_J(t-1)(1-\delta_K)^{10} + 10\times I_J(t-1),\ K_J(0)$ given

(A.10) $c_J^E(t) = q(t) + mkup_J^E$

(A.11) $CumC(t) = CumC(t-1) + 10\times E(t)$

$E(t) = \sum_J E_J(t)$

(A.12) $q(t) = \xi_1 + \xi_2\left[CumC(t)/_{CMAX}\right]^{\xi_3}$

(A.13) $LU_J(t) = LU_J(0)(1-\delta_{LU})$

$ET(t) = \sum_J(E_J(t) + LU_J(t)) + TBE\,(t)$

$TBE\,(t) = (\tau_1 + \tau_2\gamma)(t + \tau_3 t^2)$

(A.14) $M(t) = 10\times ET(t-1) + \phi_{11}M(t-1) + \phi_{21}M_U(t-1),\ M(0)$ given

$M_U(t) = \phi_{12}M(t-1) + \phi_{22}M_U(t-1) + \phi_{32}M_L(t-1),\ M_U(0)$ given

$M_L(t) = \phi_{23}M_U(t-1) + \phi_{33}M_L(t-1),\ M_L(0)$ given

(A.15) $F(t) = \eta\left\{\ln[M(t)/M^{PI}]/\ln(2)\right\} + O(t)$

$O(t) = -0.1965 + 0.13465t \qquad t \le 10$

$\quad = 1.15 \qquad t > 10$

(A.16) $T(t) = T(t-1) + \sigma_1\left\{F(t) - \frac{\eta}{\kappa}T(t-1) - \sigma_2[T(t-1) - T_L(t-1)]\right\},\ T(0)$ given

$T_L(t) = T_L(t-1) + \sigma_3[T(t-1) - T_L(t-1)],\ T_L(0)$ given

$\kappa = 1.2/f$

(A.17) $D_J(t) = \theta_{1,J}T(t) + \theta_{2,J}T(t)^2$

(A.18) $\Omega_J(t) = 1/\left[1 + D_J(t)\right]$

List of variables and parameters

Exogenous variables and parameters	
$L_J(t)$	Population (millions)
$R(t)$	Social time preference discount factor
ρ	Social time preference discount rate
α	Elasticity of output w. r. t. capital
β_J	Elasticity of output w. r. t. energy services
$A_J(t)$	Total factor productivity (TFP)
$g_J^L(t)$	Population growth rate (per decade)
$g_J^L(0)$	Population growth rate in initial period
$\delta_J^L(t)$	Rate of decline of $g^L(t)$
$g_J^A(t)$	TFP growth rate (per decade)
$g_J^A(0)$	TFP growth rate in initial period
$\delta_J^A(t)$	Rate of decline of $g^A(t)$ (per decade)
SS_J^A	Steady-state level of TFP (2005 = 1)
$Z_J(t)$	Energy efficiency
$Z_J(0)$	Energy efficiency in initial period
$g_J^Z(t)$	Energy efficiency improvement rate (per decade)
$g_J^Z(0)$	Energy efficiency improvement rate in initial period
SS_J^Z	Steady-state level of energy efficiency (2005 = 1)
$\delta_J^A(t)$	Rate of decline of $g^Z(t)$ (per decade)
δ_K	Rate of depreciation of capital (per year)
$K_J(0)$	Initial capital stock
$mkup_J^E$	Carbon services markup (1000 USD (1990) per ton carbon)
ξ_1	Marginal cost of carbon extraction in 1995
ξ_2, ξ_3	Parameters in cost-of-extraction function
$CMAX$	Point of diminishing returns in carbon extraction (GtC)
$LU_J(t)$	CO_2 emissions from land-use changes (GtC per year)
$LU_J(0)$	Emissions from land-use changes in initial period
δ_{LU}	Rate of decline of $LU_J(t)$ (per decade)
$TBE\,(t)$	Emissions due to the terrestrial biosphere effect
τ_1, τ_2, τ_3	Parameters in terrestrial biosphere process
γ	Random term in terrestrial biosphere process
η	Increase in forcing due to doubling of CO_2 concentrations
κ	Climate sensitivity parameter
f	Parameter in the process generating κ (Roe and Baker)
σ_1	Speed of adjustment for atmospheric temperature
σ_2	Coefficient of heat loss from atmosphere to deep oceans
σ_3	Coefficient of heat gain from atmosphere to deep oceans
$\theta_{1,J}$	Coefficient on linear component in damage function
$\theta_{2,J}$	Coefficient on quadratic component in damage function
Initial conditions (temperatures relative to 1900):	
$M(0)$	Initial stock of carbon in the atmosphere (GtC)
$M_U(0)$	Initial stock of carbon in the upper ocean (GtC)
$M_L(0)$	Initial stock of carbon in lower ocean (GtC)
M^{PI}	Preindustrial stock of carbon in atmosphere (GtC)
$T(0)$	Initial atmospheric temperature (°C)
$T_L(0)$	Initial ocean temperature (°C)

Carbon cycle transition coefficients (percent per decade):	
ϕ_{11}	Atmospere to atmosphere
ϕ_{12}	Atmosphere to upper box
ϕ_{21}	Upper box to atmosphere
ϕ_{22}	Upper box to upper box
ϕ_{23}	Upper box to lower box
ϕ_{32}	Lower box to upper box
ϕ_{33}	Lower box to lower box
Endogenous variables:	
W_J	(Regional) Welfare
$U_J(t)$	(Regional) Utility
$c_J(t)$	Per-capita consumption
$Q_J(t)$	Output (trillion 1990 USD per year)
$K_J(t)$	Capital stock (trillion 1990 USD)
$ES_J(t)$	Energy services from fossil fuels (GtC per year)
$E_J(t)$	Industrial CO_2 emissions (GtC per year)
$C_J(t)$	Consumption (trillion 1990 USD per year)
$I_J(t)$	Investment (trillion 1990 USD per year)
$q(t)$	World market price of carbon energy
$CumC(t)$	Cumulative industrial carbon emissions (GtC)
$ET(t)$	Total global carbon emissions (GtC per year)
$M(t)$	Atmospheric CO_2 concentration (GtC)
$M_U(t)$	CO_2 stock in the upper oceans and biosphere (GtC)
$M_L(t)$	CO_2 stock in the upper oceans (GtC)
$F(t)$	Increase in forcing relative to preindustrial (W/m^2)
$T(t)$	Atmospheric temperature increase since 1900 (°C)
$T_L(t)$	Temperature increase in lower oceans since 1900 (°C)
$D_J(t)$	Climate change damages (proportion of output)

Table 1: Global parameters: updated values and imposed uncertainty

name	original value	updated value	standard deviation[1]
ρ	3.00	—	0.33
ξ_2	700	—	140
ξ_3	4.00	—	0.80
$CMAX$	6000	—	1200
γ	—	[2]	[2]
f	—	0.65	0.10[3]
κ	2.9078	[4]	[4]
$M(0)$	735	811	—
$M_U(0)$	781	820	—
$T(0)$	0.43	0.71	—

[1] *Probability distributions are standard normals unless indicated.*

[2] *Distributed as Beta(1.5, 3.5), which gives a mean value of 0.3.*

[3] *The distribution is truncated in the right tail; see discussion in Section 3 above.*

[4] *See discussion in Section 3 and Figure 4 above.*

Table 2: Unchanged and deterministic global parameters

name	value	name	value	name	value
α	0.30	η	4.10	ϕ_{11}	0.66616
δ_K	0.10	σ_1	0.226	ϕ_{12}	0.33384
ξ_1	113	σ_2	0.440	ϕ_{21}	0.27607
δ_{LU}	0.10	σ_3	0.02	ϕ_{22}	0.60897
τ_1	0.07	$M_L(0)$	19230	ϕ_{23}	0.11496
τ_2	0.64	M^{PI}	596.4	ϕ_{32}	0.00422
τ_3	0.10	$T_L(0)$	0.06	ϕ_{33}	0.99578

Table 3: Regional parameters: updated values and imposed uncertainty

name	USA	EUR	OHI	REE	MI	LMI	CHI	LI
$LU_J(0)$	0	0	0	0	.40	.35	.05	1.00
	(0)	(0)	(0)	(0)	(.058)	(.05)	(.0083)	(.15)
$L_J(0)$	298.2	397.1	203.6	327.4	351.9	663.1	1315.8	2906.5
	(–)	(–)	(–)	(–)	(–)	(–)	(–)	(–)
$g_J^L(0)$	0.0989	-0.0126*	-0.0082*	-0.0427	0.1453	0.1312	-0.0287*	0.1960
	(0.0045)	(0.0234)	(0.0227)	(0.0046)	(0.0054)	(0.0056)	(0.0277)	(0.0052)
δ_J^L	0.2223	0.15	0.15	0.1566	0.3652	0.3148	0.15	0.23
	(0.075)	(0.05)	(0.05)	(0.05)	(0.09)	(0.09)	(0.05)	(0.0506)
$g_J^A(0)$	28.46	27.72	22.23	50.00	21.49	19.65	67.81	33.05
	(3.36)	(2.24)	(11.42)	(10.00)	(13.71)	(8.57)	(8.63)	(4.85)
SS_J^A	12.60	15.38	13.46	15.64	14.39	11.52	20.09	20.09
	(0.79)	(0.72)	(0.95)	(0.32)	(1.55)	(1.08)	(10.52)	(1.67)
$g_J^Z(0)$	-0.2340	-0.1821	-0.0183	-0.2657	-0.1454	-0.1002	-0.2459	-0.1459
	(0.1022)	(0.0046)	(0.0043)	(0.1219)	(0.1399)	(0.0489)	(0.1123)	(0.0712)
SS_J^Z	0.2706	0.2019	0.0838	0.0973	0.2592	0.1818	0.0064	0.2479
	(0.1193)	(0.0614)	(0.001)	(0.0865)	(0.15)	(0.15)	(0.1218)	(0.15)
β_J	0.091	0.057	0.059	0.08	0.087	0.053	0.096	0.074
	(– – – – – – – – – – – – – – – – – – *20% of the mean value* – – – – – – – – – – – – – – – – – –)							
$mkup_J^E$	300.0	400.0	350.0	-38.12	250.0	-2.63	-41.09	18.78
	(–)	(–)	(–)	(–)	(–)	(–)	(–)	(–)
$\theta_{J,1}$	-0.0026	-0.001	-0.007	-0.0076	-0.0039	-0.0022	-0.0041	.01
	(– – – – – – – – – – – – – – – – – – *20% of the mean value* – – – – – – – – – – – – – – – – – –)							
$\theta_{J,2}$	0.0017	0.0049	0.003	0.0025	0.0013	0.0026	0.002	0.0027
	(– – – – – – – – – – – – – – – – – – *20% of the mean value* – – – – – – – – – – – – – – – – – –)							

Mean values are reported, standard deviations (where applicable) in parentheses. The values of $L_J(0)$, $g_J^L(0)$ and $g_J^A(0)$ have been updated; original values are not reported. All parameters follow normal distributions, truncated when necessary. All rates are per decade.

* *"Initial" growth rates here refers to 2045, see Section 3 for details.*

References

[1] Sir P. Dasgupta, "Comments on the Stern Review's Economics of Climate Change", *National Institute Economic Review* 199: 4–7, 2007.

[2] Friedlingstein. P. *et al.* "Climate-Carbon Cycle Feedback Analysis, Results from the C4MIP Model Intercomparison", *Journal of Climate* 19(14): 3337–3353, 2006.

[3] Heston, A., Summers, R., and Aten, B., *Penn World Table Version 6.1*, Center for International Comparisons at the University of Pennsylvania (CICUP), October 2002.

[4] Hope, C., "The Marginal Impact of CO_2 from PAGE2002: An Integrated Assessment Model Incorporating the IPCC's Five Reasons for Concern" , *Integrated Assessment Journal* 6: 19–56, 2006.

[5] IPCC, *Climate Change 2001: The Third Assessment Report of the Intergovernmental Panel on Climate Change*, Cambridge Univ. Press, Cambridge, 2001

[6] IPCC, *Climate Change 2007: The Fourth Assessment Report of the Intergovernmental Panel on Climate Change*, Cambridge Univ. Press, Cambridge, 2007

[7] Mastrandrea, M. D., and Schneider, S. H., "Probabilistic Integrated Assessment of "Dangerous" Climate Change", *Science* 304: 571–575, 2004.

[8] McKibbin, W. J., Pearce, D. and Stegman, A., "Can the IPCC SRES Be Improved?", *Energy & Environment* 15(3): 359–360, 2004.

[9] Murphy, J. *et al.* "Quantification of Modelling Uncertainties in a Large Ensemble of Climate Change Simulations" , *Nature* 430: 768–772, 2004.

[10] Nakićenović, N. *et al. Emission Scenarios. A Special Report of Working Group III of the Intergovernmental Panel on Climate Change,* Cambridge Univ. Press, Cambridge, U. K., 2000.

[11] Nordhaus, W. D., "The Stern Review on the Economics of Climate Change" , Mimeographed, Yale University, November 2006.

[12] Nordhaus, W. D. and Boyer, J., *Warming the World: Economic Models of Global Warming*, MIT Press, Cambridge, MA, 2000.

[13] Nordhaus, W. D. and Popp, D., "What is the Value of Scientific Knowledge", *The Energy Journal* 18: 1–45, 1997.

[14] Roe, G. H. and Baker, M. B., "Why Is Climate Sensitivity So Unpredictable" , *Science* 318: 629–632, 2007.

[15] Schenk, N. J. and Lensink, S. M., "Communicating Uncertainty in the IPCC's Greenhouse Gas Emissions Scenarios", *Climatic Change* 82: 293–308, 2007.

[16] Sir N. Stern (ed), *The Stern Review on the Economics of Climate Change*, Cambridge Univ. Press, Cambridge, 2006.

[17] Webster, M. D. *et al.* "Uncertainty in Emissions Projections for Climate Models", *Atmospheric Environment* 36: 3659–3670, 2002.

[18] Weitzman, M., in press, "The Stern Review of the Economics of Climate Change", *Journal of Economic Literature*.

[19] Wigley, T. M. L. and Raper, S. C. B., "Interpretation of High Projections for Global-Mean Warming" , *Science* 293: 451–454, 2001.